

Backpropagation through space, time, and the brain

Benjamin Ellenberger*, Paul Haider*,
Jakob Jordan, Kevin Max, Ismael Jaras, Laura Kriener, Federico Benitez,
Mihai A. Petrovici

*Shared first authorship

Department of Physiology, University of Bern, 3012 Bern, Switzerland.

Abstract

Effective learning in neuronal networks requires the adaptation of individual synapses given their relative contribution to solving a task. However, physical neuronal systems – whether biological or artificial – are constrained by spatio-temporal locality. In other words, synapses can only use information available at their physical location and at the same moment in time as the synaptic updates themselves. How such networks can perform efficient credit assignment, remains, to a large extent, an open question. In Machine Learning, the answer is almost universally given by the error backpropagation algorithm, through both space (BP) and time (BPTT). However, BP(TT) is well-known to rely on biologically implausible assumptions, in particular with respect to spatiotemporal (non-)locality, while forward-propagation models such as real-time recurrent learning (RTRL) suffer from prohibitive memory constraints. We introduce Generalized Latent Equilibrium (GLE), a computational framework for fully local spatio-temporal credit assignment in physical, dynamical networks of neurons. We start by defining an energy based on neuron-local mismatches, from which we derive both neuronal dynamics via stationarity and parameter dynamics via gradient descent. The resulting dynamics can be interpreted as a real-time, biologically plausible approximation of BPTT in deep cortical networks with continuous-time neuronal dynamics and continuously active, local synaptic plasticity. In particular, GLE exploits the ability of biological neurons to phase-shift their output rate with respect to their membrane potential, which is essential in both directions of information propagation. For the forward computation, it enables the mapping of time-continuous inputs to neuronal space, performing an effective spatiotemporal convolution. For the backward computation, it permits the temporal inversion of feedback signals, which consequently approximate the adjoint states necessary for useful parameter updates.

1 Introduction

The world in which we live is rich and regular enough to sustain systems that can learn about it. Yet, it is also a complex and dynamic environment requiring continuous, real-time learning. In the context of neural networks, such learning involves changing the parameters of the network to improve some objective function (or equivalently, reduce an objective cost). One can see the general problem of learning as that of *constrained minimization*, i.e., to minimize a cost function with respect to the parameters θ that describe the network, under constraints given by the physical characteristics of the network. For example, in the case of biological neuronal¹ networks, such dynamical constraints often include leaky integrator membranes and nonlinear output filters.

The standard approach to this problem uses stochastic gradient descent, coupled with some type of automatic differentiation algorithm that calculates gradients via reverse accumulation [1, 2]. These methods are efficient in their use of resources, and flexible in their range of applications. In cases where what is being learned is time-independent, or can be represented as a time-independent problem, the celebrated backpropagation algorithm provides this efficient backward differentiation [3–5]. We can refer to this class of problems as *spatial*, as opposed to more complex *spatio-temporal* problems, such as sequence learning. For the latter, the solution to constrained minimization can be sought by means of a variety of methods. When the dynamics are discrete, the most successful method is backpropagation through time (BPTT) [6,

¹We use the term *neuronal* to differentiate between physical dynamical networks of neurons and their abstract, artificial *neural* network (ANN) counterparts.

7]. For continuous-time problems, there is a family of related methods stemming from optimization theory, the most prominent being the adjoint method (AM) [8], Pontryagin’s maximum principle [9, 10], and the Bellman equation [11].

AM and BPTT have proven to be very powerful methods, but it is not clear how they could be implemented in physical neuronal systems that need to function and learn continuously, in real time, and using only information that is locally available at the constituent components. AM/BPTT cannot be performed in real time, as it is only at the end of a task that errors are calculated retrospectively. This implies the need to either (i) store the whole dynamics until an update time, and only then perform backward error propagation, which is difficult to reconcile with physical neuronal systems, or (ii) be able to reliably predict the future behavior of the network, which is difficult for more fundamental reasons. Additionally, it is unclear how errors are supposed to be calculated and transmitted in the first place, i.e., how to define errors that correctly account for the ongoing dynamics of the system. It is for these reasons that AM/BPTT sits firmly within the domain of machine learning, and is considered irrelevant for physical neuronal systems (carbon and silicon alike). Instead, theories of bio(-inspired) spatio-temporal learning focus on other methods, either by using reservoirs and foregoing the learning of deep weights altogether, or by using direct, global error feedback as in the case of FORCE [12] and FOLLOW [13]. Alternatively, errors can also be carried forward in time and associated with past network states, as in real-time recurrent learning (RTRL) and its many approximations [14]. We will return to these methods in the discussion, as our main focus here is AM/BPTT.

Indeed, and contrary to prior belief, we suggest that physical neuronal systems can approximate AM/BPTT very efficiently and with excellent functional performance. More specifically, we propose the overarching principle of *General Latent Equilibrium* (GLE) to derive a comprehensive set of equations for inference and learning that are local in both time and space. These equations fully describe a dynamical system running in continuous time, without the need for separate phases, and undergoing only local interactions. Moreover, they describe the dynamics and morphology of structured neurons performing both *retrospective* and *prospective* coding, as well as the weight dynamics of error-correcting synapses, thus linking to experimental observations of cortical dynamics and anatomy. Due to its manifest locality and reliance on rather conventional analog components, our framework also suggests a blueprint for powerful and efficient neuromorphic implementation.

We thus propose a new solution for the spatio-temporal credit assignment problem in physical neuronal systems, with important advantages over previously proposed alternatives. In Fig. 1 we present an intuitive picture of the relationship between GLE and previous methods of spatio-temporal error propagation. Importantly, our framework does not differentiate between spatial and temporal tasks and can thus be readily used in both domains. As it represents a generalization of Latent Equilibrium (LE) [15], it implicitly contains BP as a sub-case.

This manuscript is structured as follows: In Section 2.1, we propose a set of four postulates from which we derive network structure and dynamics. This approach is strongly inspired by approaches in theoretical physics, where a specific energy function provides a unique reference from which everything else follows. The derivation of network dynamics, is made explicit in Section 2.2. In Section 2.3 we discuss how these dynamics effectively implement an approximation of AM/BPTT, and we also show how these describe physical networks of neurons, with implications for both cortex and hardware (Section 2.4). Finally, in Section 3, we discuss various applications, from very small-scale setups that allow an intuitive understanding of our framework, to larger-scale networks for difficult spatio-temporal classification problems. Finally, we discuss the connections and advantages of our framework when compared to other approaches in Section 4.

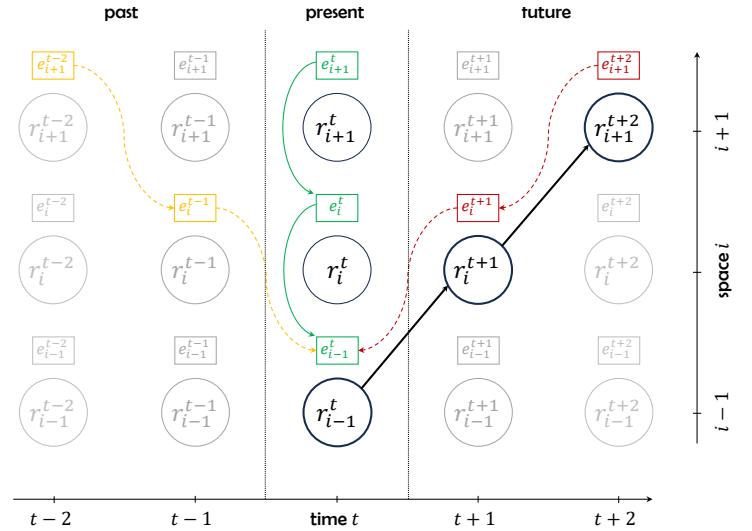


Figure 1: Comparison between GLE and other methods for temporal processing in layered neural networks. Red: **BPTT** effectively uses future errors $e(t + \Delta t)$ and present neuronal states $r(t)$ for parameter updates; therefore, it can only be implemented in an offline fashion. Yellow: **RTRL** stores past states $r(t - \Delta t)$ to learn using the errors at the present moment $e(t)$; for large networks, the memory overhead becomes intractable. Green: **GLE** operates exclusively on present states $r(t)$ and errors $e(t)$; it uses them to infer the future errors, thus enabling an efficient approximation of BPTT.

2 Theory

2.1 The GLE framework

At the core of our framework is the realization that biological neurons are capable of performing two fundamental temporal operations. First, as is well-known, neurons perform temporal integration in the form of low-pass filtering. We describe this as a “retrospective” operation, as it is a function of past inputs, and denote it with the operator

$$\mathcal{I}_{\tau^m}^- \{x(t)\} := \int_{-\infty}^t x(s) \exp\left(-\frac{s-t}{\tau^m}\right) ds, \quad (1)$$

where τ represents the membrane time constant and x the synaptic input.

The second temporal operation is much less known but well-established physiologically [16–20]: neurons are capable of performing temporal differentiation, an inverse low-pass filtering that shifts inputs into the future, and which we thus name “prospective” and denote with the operator

$$\mathcal{D}_{\tau^r}^+ \{x(t)\} := \left(1 + \tau^r \frac{d}{dt}\right) x(t) \quad (2)$$

with τ^r a time constant associated with the neuronal output rate, which, rather than being simply $\varphi(u)$ (with u the membrane voltage and φ the neuronal activation function), takes on the prospective form $r = \varphi(\mathcal{D}_{\tau^r}^+ \{u\})$.

In brief, this prospectivity can arise from two distinct mechanisms. On shorter time scales, it represents a direct consequence of the output nonlinearity [18, 20]. On longer time scales, it follows from slower adaptive processes in the neuron, for example spike-frequency adaptation [19]. For negative adaptation coupling, the adaptation current can act as a subtractive low-pass filter, thus approximating a high-pass filter and thereby, in turn, the inverse low-pass operation described above [21, 22]. Also in analog neuromorphic hardware, adaptive neurons are readily available (e.g., [23]), but the direct implementation of an inverse low-pass filter is, of course, even more simple and efficient.

Importantly, these two operators have opposite effects; in particular, for $\tau^m = \tau^r$, they are exactly inverse, which forms the basis of Latent Equilibrium (LE) [15]. In that case, the exact inversion of the low-pass filtering allows the network to react instantaneously to a given input, which can solve the relaxation problem for spatial tasks. However, this exact inversion also precludes the use of neurons for explicit temporal processing in spatio-temporal tasks, which represents the main focus of this work.

We can now define the GLE framework as a set of four postulates, from which the entire network structure and dynamics follow. The postulates use these operators to describe how forward and backward prospectivity work in biological neuronal networks, and also how they approximate adjoint equations without the need for learning phases.

Postulate 1. *The canonical variables describing neuronal network dynamics are $\mathcal{D}_{\tau^m}^+ \{u(t)\}$ and $\mathcal{D}_{\tau^r}^+ \{u(t)\}$.*

This determines the relevant dynamical variables for the postulates below. They represent, respectively, the prospective voltages with respect to the membrane and rate time constants. The output rate of a neuron in terms of these quantities and their inverses is simply $r(t) = \varphi(\mathcal{D}_{\tau^r}^+ \{u(t)\}) = \varphi(\mathcal{D}_{\tau^r}^+ \{\mathcal{I}_{\tau^m}^- \{I(t)\}\})$. In other words, a neuron does these two operations consecutively: first, it low-pass-filters its input, then it inverse-low-pass-filters it to produce an output. Importantly, the time constants of these two processes are not necessarily identical.

Postulate 2. *A neuronal network is fully described by an energy function*

$$E(t) = \frac{1}{2} \|e_i(t)\|^2 = \frac{1}{2} \sum_i \|\mathcal{D}_{\tau^m}^+ \{u_i(t)\} - \sum_j W_{ij} \varphi(\mathcal{D}_{\tau^r}^+ \{u_j(t)\}) - b_i\|^2 + \beta C(t), \quad (3)$$

where W_{ij} and b_i respectively represent the weight matrix and bias vector, and the cost function $C(t)$ is scaled by a factor β . The cost can be defined as a function of the prospective membrane voltage $\mathcal{D}_{\tau^m}^+ \{u_i(t)\}$ of some subset of output neurons, or as a function of their rate, and hence of $\mathcal{D}_{\tau^r}^+ \{u_j(t)\}$.

This approach is inspired by physics and follows a time-honored tradition in machine learning and computational neuroscience [15, 24–26]. As in LE, under the weak assumption that the cost function can be factorized, this energy is

simply a sum over neuron-local energies $E_i(t) = \frac{1}{2}e_i^2(t) + \beta C_i(t)$. Each of these energies represent a difference between what membrane voltage the neuron predicts for its near future ($\mathcal{D}_{\tau^m}^+ \{u_i(t)\}$), and what its functional afferents (and bias) expect it to be ($\sum_j W_{ij} \varphi(\mathcal{D}_{\tau^r}^+ \{u_j(t)\})$), with the potential addition of a nudging term that is related to the cost that the network wants to minimize ($\beta C_i(t)$).

Postulate 3. *Neuron dynamics follow the stationarity principle*

$$\mathcal{I}_{\tau^m}^- \left\{ \frac{\partial E}{\partial \mathcal{D}_{\tau^m}^+ \{u_i\}} \right\} + \mathcal{I}_{\tau^r}^- \left\{ \frac{\partial E}{\partial \mathcal{D}_{\tau^r}^+ \{u_i\}} \right\} = 0. \quad (4)$$

Intuitively speaking, the two rates of change (the partial derivatives) are prospective, with temporal advances determined by τ^m and τ^r , so they are estimators for quantities that exist at different points in time (roughly speaking, at $t + \tau^m$ and $t + \tau^r$). To compare the two rates of change on equal footing, they need to be pulled back into the present by their respective inverse operators $\mathcal{I}_{\tau^m}^-$ and $\mathcal{I}_{\tau^r}^-$. It is the equilibrium of this mathematical object, otherwise not immediately apparent (hence: “latent”) from observing the network dynamics themselves (see below), that gives our framework its name. It is also easy to check that for the special case of $\tau^m = \tau^r$, GLE reduces to LE [15] – hence the ‘generalized’ nomenclature.

Postulate 4. *Parameter dynamics follow gradient descent on the energy*

$$\dot{\boldsymbol{\theta}} = -\eta_{\boldsymbol{\theta}} \frac{\partial E}{\partial \boldsymbol{\theta}}. \quad (5)$$

Parameters include $\boldsymbol{\theta} = \{\mathbf{W}, \mathbf{b}, \boldsymbol{\tau}^m, \boldsymbol{\tau}^r\}$, with boldface denoting matrices, vectors, and vector-valued functions.

These four postulates fully encapsulate the GLE framework. From here, we can now take a closer look at the network dynamics and see how they enable the sought transport of signals to the right place and at the right time.

2.2 Network dynamics

In the following, for better readability, we repeatedly use bars and breves as shorthand notations for retrospective and prospective operations respectively; for example, $\bar{x}^m := \mathcal{I}_{\tau^m}^- \{x\}$ and $\check{x}^r := \mathcal{D}_{\tau^r}^+ \{x\}$.

With our postulates at hand, we can now derive the neuronal dynamics by applying Eqn. (4) to the energy function defined by Eqn. (3):

$$\tau_i^m \dot{u}_i = -u_i + \sum_j W_{ij} \varphi(\check{u}_j^r) + b_i + e_i. \quad (6)$$

This is very similar to conventional rate dynamics, except for the use of the prospective operator for the neuronal output, which we already connected to the dynamics of biological neurons above. Thus, in the GLE framework, a single neuron performs three operations in the following order: integration (retrospective), differentiation (prospective), and the output nonlinearity. The timescale associated with retrospectivity is the membrane time constant τ^m , whereas prospectivity is governed by τ^r . This means that even for fixed membrane time constants (as is often the case for biological neurons), single neurons can tune the time window to which they attend by modifying their prospectivity. This temporal attention window can lie in the past (retrospective neurons, $\tau^r < \tau^m$), in the present (instantaneous neurons, $\tau^r = \tau^m$, described by LE), but also in the future (prospective neurons, $\tau^r > \tau^m$). These neuron classes can, for example, be found in cortex [27, 28] and hippocampus [29, 30]; for a corresponding modeling study, we refer to [20]. This prospective capability becomes essential for error propagation, as we discuss below, while the use of different attention windows allows the learning of complex spatio-temporal patterns, as we show in action in Section 3. Note that for $\tau^r = 0$, we recover classical leaky integrator neurons as a special case of our framework.

Eqn. (6) also suggests a straightforward interpretation of neuronal morphology and its associated functionality. In particular, it suggests that separate neuronal compartments store different variables: a soma compartment for the voltage u_i , and dendritic compartments for integrating $\sum_j W_{ij} r_j$ and e_i . This separation also gives synapses access to these quantities, as we discuss later on. Further below, we also show how this basic picture extends to a micro-circuit for learning and adaptation in GLE networks.

The error terms in GLE also naturally include prospective and retrospective operators. As we postulate above (Eqn. (3)), the total energy of the system is defined as the sum of all the individual error terms. If we consider a hierarchical network, these terms can be rearranged into the form

$$e_\ell = \mathcal{D}_{\tau^m}^+ \{ \mathcal{I}_{\tau^r}^- \{ \varphi'_\ell \odot \mathbf{W}_{\ell+1}^T e_{\ell+1} \} \} , \quad (7)$$

where ℓ denotes the network layer and φ' denotes the derivative of φ evaluated at \check{u}^r . For $\tau^r = \tau^m$, the operators cancel and this reduces to the well-known error backpropagation algorithm, as already studied in LE. In GLE however, this error term exhibits a temporal inversion. Whereas forward rates are retrospective with timescale τ^m and prospective with τ^r , backward errors invert this relationship. As we discuss in the following section, it is precisely this inversion that enables the approximation of AM/BPTT.

Finally, the parameter dynamics are obtained from Eqn. (5). For example, synaptic plasticity follows

$$\dot{W}_{ij} = \eta_W e_i r_j = \eta_W (\check{u}_i^m - v_i) r_j , \quad (8)$$

where $v_i = \sum_j W_{ij} r_j$ is a dendritic compartment that integrates multiple synaptic inputs. Such three-factor error-correcting rules represent a de-facto standard; for a more detailed biological description, we refer to [31]. Notice that parameter learning is neuron-local, and that we are performing gradient descent explicitly on the energy E , and only implicitly on the cost C . The locality of GLE dynamics is thus a direct consequence of the locality of the postulated energy function and provides the physical and biological plausibility that other methods lack. In Section 2.4, we discuss how GLE dynamics relate to physical neuronal networks and cortical circuits, but first we show how these dynamics effectively approximate AM/BPTT.

2.3 GLE dynamics implement a real-time approximation of AM/BPTT

The inclusion of neuronal prospectivity in our framework represents the key ingredient for its learning capabilities: GLE constitutes a real-time, online approximation of the adjoint method. This property can be best seen by directly comparing the learning equations for GLE and AM. In the simplest one-layer case with presynaptic input $r_{\text{in}}(t)$, the two learning rules read:

$$\dot{W}_{\text{AM}}(t) \propto \mathcal{I}_{\tau^m}^+ \{ \mathcal{D}_{\tau^r}^- \{ \varphi' \odot (r^* - r) \} \} \otimes r_{\text{in}}(t) \quad (9)$$

$$\dot{W}_{\text{GLE}}(t) \propto \mathcal{D}_{\tau^m}^+ \{ \mathcal{I}_{\tau^r}^- \{ \varphi' \odot (r^* - r) \} \} \otimes r_{\text{in}}(t). \quad (10)$$

Notice the use of adjoint operators $\mathcal{D}_\tau^-[x(t)] = (1 - \tau \frac{d}{dt}) x(t)$ and $\mathcal{I}_\tau^+[x(t)] = \frac{1}{\tau} \int_t^\infty ds x(s) e^{\frac{s-t}{\tau}}$ in the error terms. These two expressions are obviously not identical, and in particular the operator $\mathcal{I}_{\tau^m}^+$ in AM assumes a knowledge of the future that is impossible for an online method such as GLE. However, the concatenation of the two operators in AM and GLE *does* lead to a very useful approximation, as we show below.

The best way to see this is in frequency space, where we can analyze how these operators filter an individual frequency component. In Fourier space, the relevant operators can be written as follows:

$$\mathcal{D}_{\tau^r}^- = 1 - i\omega\tau^r , \quad \mathcal{I}_{\tau^m}^+ = \frac{1}{1 - i\omega\tau^m} , \quad (11)$$

$$\mathcal{D}_{\tau^r}^+ = 1 + i\omega\tau^r , \quad \mathcal{I}_{\tau^m}^- = \frac{1}{1 + i\omega\tau^m} . \quad (12)$$

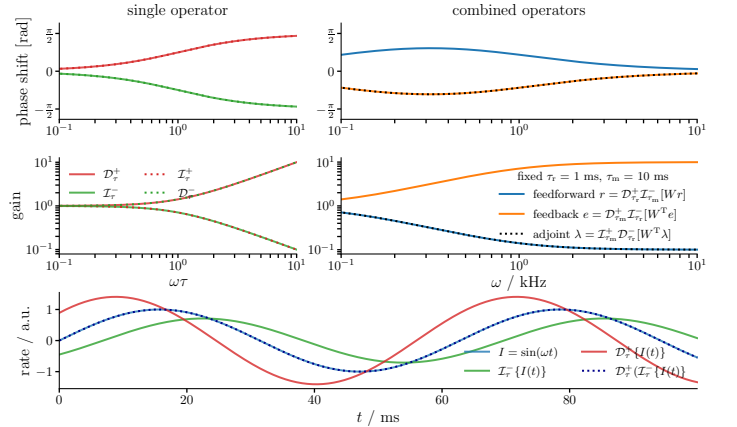


Figure 2: Comparison of GLE and Adjoint Method (AM) in Fourier space. Top four panels: effect of the four operators and their pairwise combinations as they appear in the propagation of rates (blue), errors (e , GLE, orange) and adjoint variables (λ , AM, dotted black). Note how GLE errors arrive at precisely the correct time (phase shift), albeit with different amplitude (gain). Bottom: Example trace demonstrating the exact inverse relationship between the \mathcal{I} and \mathcal{D} operators.

Treating these operators as filters, we can easily compute the gain and phase shift that they impose on a single incoming frequency component (see Fig. 2). In particular, the following relations hold:

$$\Phi_{\text{AM}} = \Phi_{\text{GLE}} \quad \text{and} \quad G_{\text{AM}} = \frac{1}{G_{\text{GLE}}}, \quad (13)$$

where Φ denotes the phase shift and G denotes the gain. This shows that in terms of temporal shift, the GLE errors are perfect replicas of the adjoint variables derived from exact gradient descent; this is the most important part of the temporal backpropagation in AM. In other words, for any frequency component, the backpropagated error has precisely the correct shift (forward) in time. In terms of gain, GLE and AM are inverted. For $\omega\tau \lesssim 1$, this approximation is very good and the gradients are only weakly distorted. Since this is the target regime for the forward propagation in the first place, the gain difference translates to a tuning of learning rates. However, even for larger $\omega\tau$, the gradients never change sign, so the error signal always remains useful.

2.4 Cortical / neuromorphic circuits

As shown above, GLE backward (error) dynamics use the same sequence of operations as those performed by forward (representation) dynamics: first \mathcal{I}_τ^- then \mathcal{D}_τ^+ . This suggests that backward errors can be transmitted by the very same type of neurons as forward signals, which is in line with substantial experimental evidence that demonstrates the encoding of errors in L2/3 pyramidal neurons [32–37]. Note that correct local error signals are only possible with neurons that are capable of both retrospective (\mathcal{I}_τ^-) and prospective (\mathcal{D}_τ^+) coding – the core element of the GLE framework.

This symmetry between representation and error suggests a simple microcircuit motif that repeats in a ladder-like fashion, with pyramidal error neurons counterposing pyramidal representation neurons (Fig. 3). The propagation of errors requires two further elements that can be implemented by static lateral synapses. First, the error neurons need to be multiplicatively gated by the same activation function φ' as their respective representation neurons. This can either happen through direct lateral interaction, or through divisive gating via inhibitory interneurons [38–41], via synapses that are appropriately positioned at the junction between dendrites and soma. The required signal can be generated and transported in different ways depending on the specific form of the activation function. For example, if $\varphi = \text{ReLU}$, lateral weights can simply be set to $\mathbf{L}^b = \mathbf{1}$. For sigmoidal activation functions, φ' can be very well approximated by synapses with short-term plasticity (e.g., [42], Eqn. 2.80).

The second requirement regards the communication of the error back to the error dendrites of the representation neurons; this is easily achieved by setting $\mathbf{L}^f = \mathbf{1}$. Comparing the figure with the theory, we can see that the latter also implies $B = W^T$. While this can, to some extent, be mitigated by feedback alignment [43], online, local and phase-free solutions for the weight transport problem have also been recently proposed [44, 45].

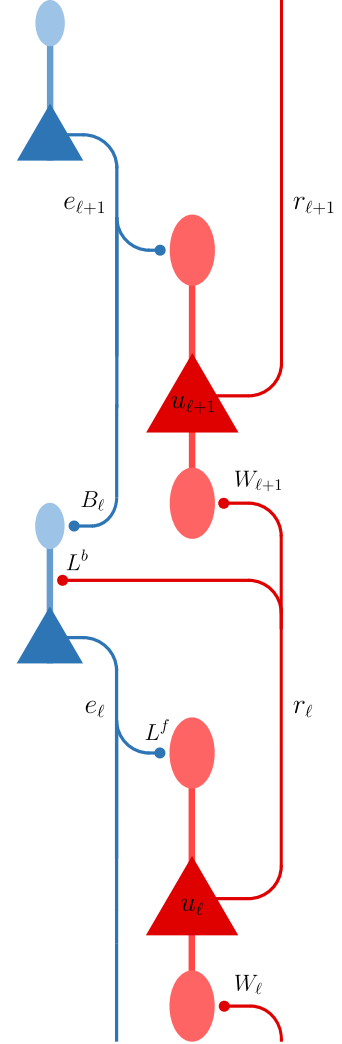


Figure 3: Microcircuit implementation of GLE. Representation neurons are depicted in red, error neurons in blue. Both classes of neurons are of the same type, here represented as pyramidal neurons. The drawn synapses provide neurons with all the necessary local information to carry out the dynamics derived from GLE, given an intrinsic capability of neurons to perform both retrospective and prospective operations.

3 Applications

In this section, we demonstrate several applications of the GLE framework. The method is very flexible and in principle able to deal with tasks of high spatio-temporal complexity. We start with small-scale demonstrations in simple networks, in order to provide an intuition of how GLE can solve non-trivial temporal tasks. Later on, we discuss more difficult problems that usually require the use of sophisticated machine learning methods and compare the performance of GLE with the most common approaches in ML.

3.1 GLE in a chain of neurons

As a first application, we study a chain of GLE neurons provided with a periodic step function input (Fig. 4). Specifically, we implement a teacher/student protocol in which a teacher chain with fixed weights provides the target output rates, and a randomly initialized student chain tries to learn the mimic task, ideally learning the teacher network’s weights and time constants.

We compare two different solutions to this problem: (1) GLE dynamics are computed online with the goal of learning the exact weights and time constants of the teacher network. (2) Only the forward dynamics are computed online, and errors are backpropagated instantaneously according to $e_i = \varphi'_i w_i e_{i+1}$ (standard BP), i.e., without inversely modulating the error signals with the GLE operators in the feedback pathway. In that case, we observe how learning of the parameters is not possible because feedback errors and presynaptic activities are not correctly aligned in time. This does not only prevent the network from converging to a good solution, but can even lead to diverging parameters, as seen here for the membrane time constants. In contrast, GLE dynamics provide good estimates of the future error signals, which correctly invert the lag in the feedforward pathway and allow the stable learning of all network parameters.

3.2 Small GLE networks

In a second setup, we conserve the network depth, but increase the size (and thereby the representational capacity) of the hidden layers (Fig. 5). We continue using a teacher/student protocol, but given the larger latent space, there usually exists more than one possible combination of weights that can reproduce the output rates of the teacher network.

Here, we directly compare GLE with the gold standard of AM. Note, however, that unlike GLE, AM is not an online method and gradients can only be computed for fixed time windows. At the end of each window, gradients can be computed by integrating the adjoint equations of the forward dynamics backwards in time, leading to a characteristic step-like evolution of the network parameters. For this reason, GLE might even have a slight advantage in terms of convergence speed when compared to AM. While in theory AM provides an exact solution to the constrained optimization problem, any numerical implementation must use finite time windows, leading to discretized learning, which might cause overshoots in the parameters that need to be corrected. In contrast, GLE’s online dynamical learning, while being only

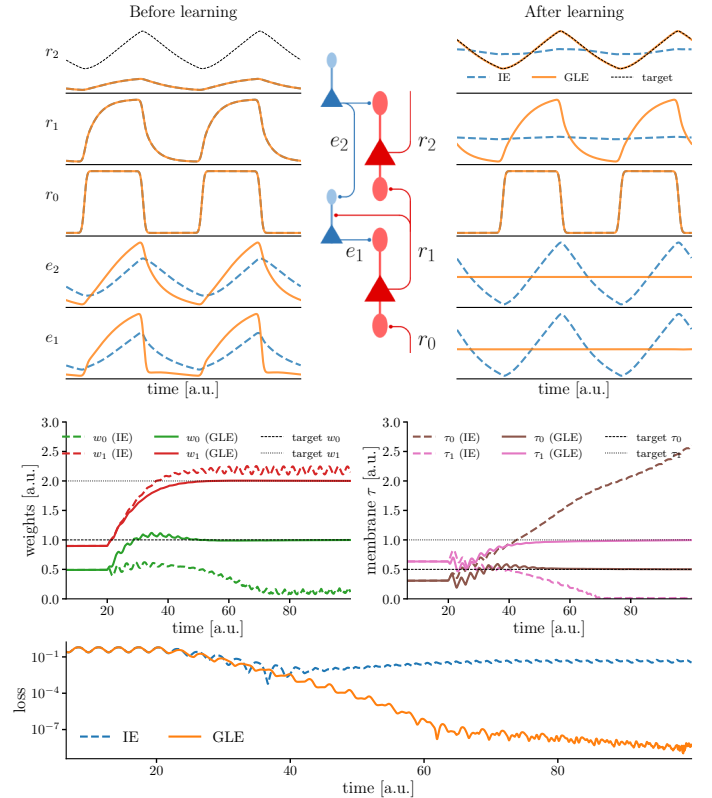


Figure 4: Learning with GLE in a simple chain. A chain of 2 GLE neurons (red) with corresponding error neurons (blue) is trained to mimic the output of a teacher network. The network structure is shown at the top, together with neuronal outputs r_i and errors e_i for the student network before (left) and after (right) learning. The middle row shows the evolution of the weights (left) and membrane time constants (right) of the student network, and the bottom row shows the evolution of the output loss. GLE learning is compared to standard backpropagation with instantaneous errors (IE). The latter fails to learn the task, as the errors are not temporally aligned with the presynaptic activities. Note that instantaneous errors are already a strong assumption and require a form of prospectivity to be realized [15]. Without prospectivity, the student network would perform even worse.

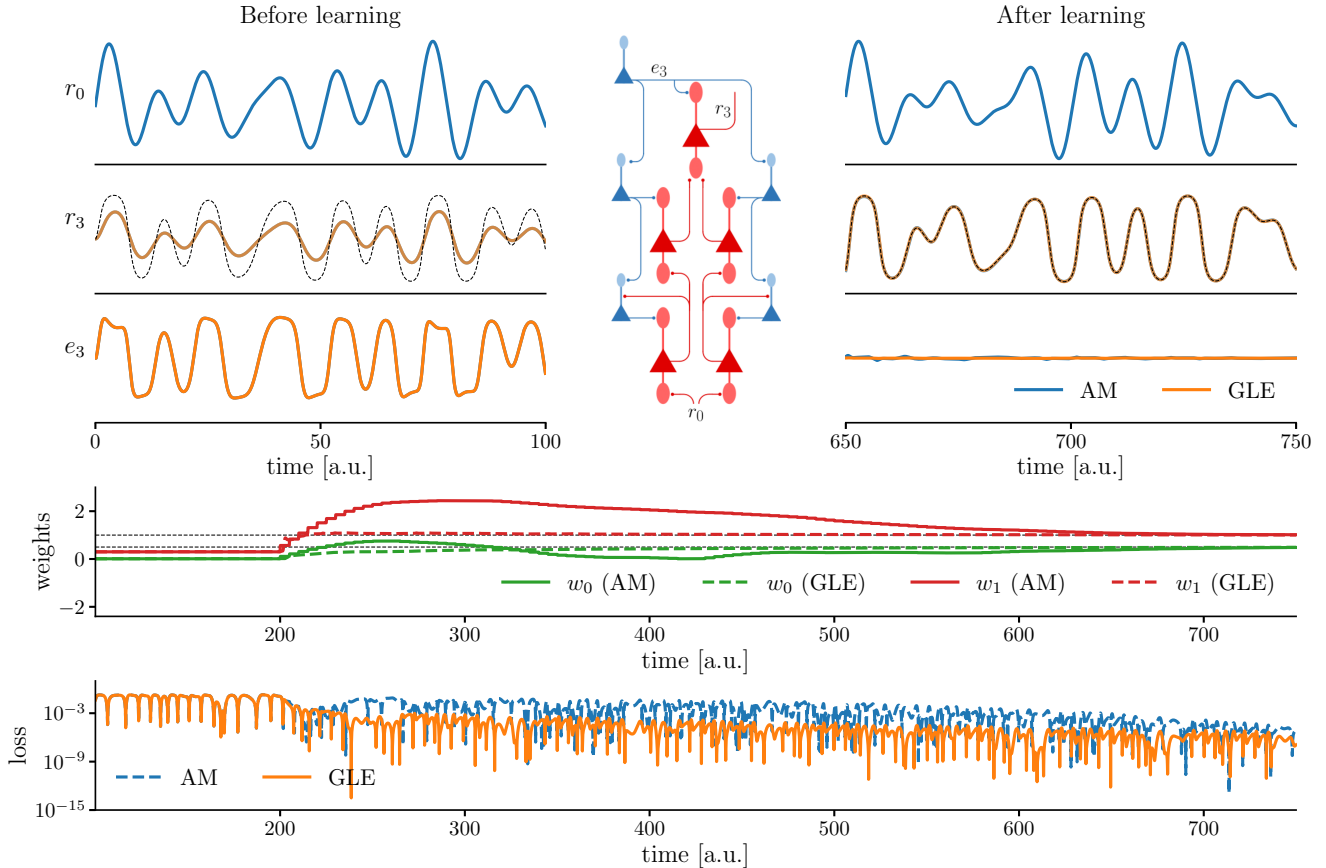


Figure 5: Learning in a small network of GLE neurons (one output neuron, two hidden layers of two neurons each). GLE performs on par with standard AM, even exhibiting an advantage in convergence speed due to its inherently online nature.

an approximation of the exact adjoint dynamics, in practice allows for a more fine-grained integration of the error signals, and therefore better convergence properties.

3.3 GLE for challenging spatiotemporal classification problems

We now demonstrate the performance of GLE in larger networks, applied to difficult spatio-temporal learning tasks.

First, we compare GLE with state-of-the-art benchmarks for MNIST-1D [46] (Fig. 6a). Other than the name itself and the number of classes, MNIST-1D bears little resemblance to its classical namesake. Here, each example is a one-dimensional sequence of points, which provides a temporal sequence as input to the network. In order to correctly classify a sample, the network must be able to store a (processed) memory of the input’s past. Unlike for networks trained with BPTT, for GLE this combination of dynamic memory, learning and classification must occur online.

In Fig. 6b, we can see how a multi-layered perceptron fails to appropriately learn to classify this dataset, reaching a validation accuracy of only around 60%. This is despite the perceptron having access to the entire data from the sample at the same time, unrolled from time into space. This highlights the difficulty of the MNIST-1D task, where the network needs to learn to neglect different kinds of temporal noise on multiple time scales [46]. More involved machine learning methods achieve much better results, with temporal convolutional networks (TCNs, [47]) and gated recurrent units (GRUs, [48]) achieving averages of over 90%. Notably, both of these methods work offline, with TCNs in particular requiring a mapping of temporal signals to spatial representations beforehand, and GRUs requiring offline BPTT training.

Because GLE networks learn fully online, they exhibit longer convergence times, as they are often confronted with counterproductive combinations of inputs and targets (3/4 of the total input in MNIST-1D is noise). Still, the prospective errors manage to provide good online approximations of the true gradients for updating the network parameters. Thus,

despite facing a significantly more difficult task compared to the methods that have access to the full network activity unrolled in time, GLE achieves highly competitive classification results.

In Fig. 6c, we show the results of GLE on the Google Speech Commands dataset [49]. This dataset consists of 105’829 one-second long audio recordings of 35 different speech commands, each spoken by thousands of people. In the v2.12 version of this dataset, the usual task is to classify 10 different speech commands in addition to a silence and an unknown class, which comprises all remaining commands. The raw audio signal is transformed into a sequence of 32 Mel spectrograms with 32 frequency bins each to make it a more salient input for classification. Similarly to the MNIST-1D dataset, the GLE network is trained online, while the other networks are trained offline, with the MLP and TCN using all temporal data unrolled into space. On this task, GLE surpasses the MLP and achieves a performance that comes close to TCN and GRU networks.

We thus conclude that the advantages of GLE in terms of biological plausibility and online learning capability come without losing its competitive edge in terms of raw task performance.

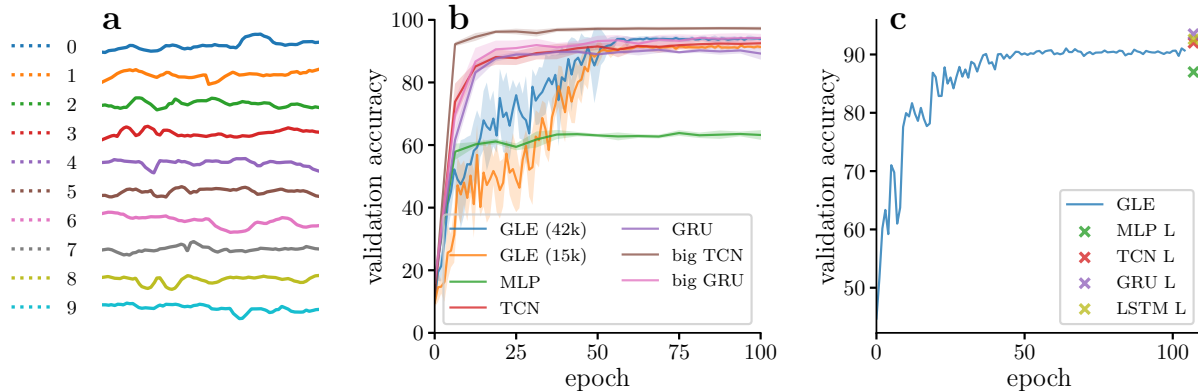


Figure 6: Comparison of GLE with powerful ML methods on two challenging spatio-temporal classification problems: In the first two panels, the MNIST1D dataset [46]. Averages and standard deviations measured over 5 seeds. In the last panel, early results from the Google Speech Commands dataset [49]. **(a)** Exemplary MNIST1D samples. **(b)** Validation accuracy. Both MLP and TCN networks are trained with spatial BP and need the temporal signal to be transformed into a spatial representation beforehand. For GRU networks, the temporal signal is processed in a streaming fashion. These networks include a readout layer that has access to all hidden states over time and is trained offline with BPTT. Our GLE networks achieve competitive performance, but with fully online training. **(c)** Validation accuracy of GLE and other methods on the Google Speech Commands dataset. The task requires the classification of spoken words from an audio signal represented by Mel spectrograms. A single sample is represented by a sequence of 32 Mel spectrograms with 32 frequency bins each. The code was taken from [50], but the networks were retrained on the newer v2.12 dataset version instead of on the v1.12 version as reported in the original publication. As in the MNIST1D dataset, both MLP and TCN networks were trained with spatial BP on a spatial representation of the temporal signal. The GRU network was trained offline with BPTT. Although the GLE network was trained online, it surpasses the MLP and achieves a performance comparable to the TCN and GRU networks.

Model	GLE (42k)	GLE (15k)	MLP	TCN	GRU	best TCN	best GRU
params	W, b	W, b	W, b	W, b	W, b	W, b	W, b
# params	42040	14956	15210	5210	5134	11960	8974
acc / %	93.9 ± 0.7	91.3 ± 0.9	64.4 ± 0.9	92.5 ± 0.8	91 ± 1	97.3 ± 0.5	94.6 ± 0.7

Table 1: Summary of the different evaluated network models and their performance on the MNIST-1D dataset.

3.4 GLE for challenging spatial classification problems

The previous results show that GLE works very well as an online approximation of AM/BPTT in the case of temporally complex tasks. But GLE is in fact more general than that as a method, and can also tackle purely spatial tasks, such as image classification. In cases like this, where temporal information is irrelevant, the most efficient strategy is to take the LE limit of GLE, i.e., $\tau^m = \tau^r$. In Fig. 7 we compare the accuracy of LE with that of classical BP on three datasets of varying complexity. Note that learning is performed in a time-continuous manner in all of these cases as well.

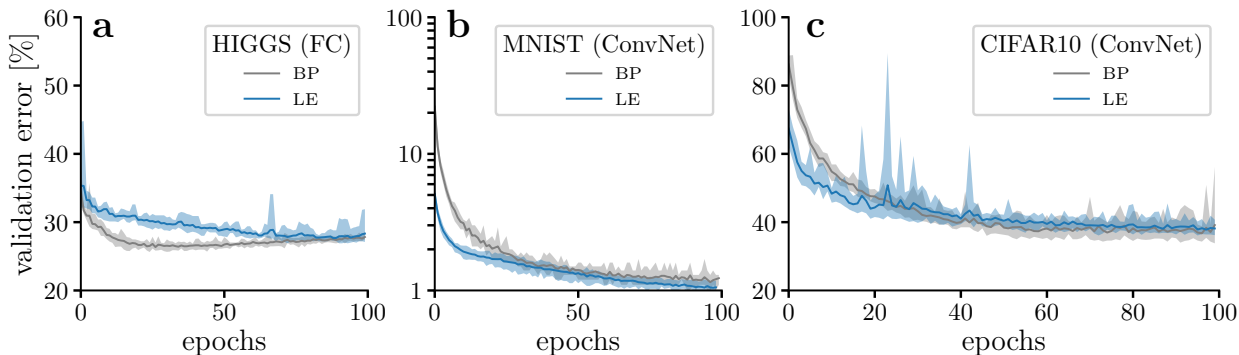


Figure 7: GLE learning of purely spatial patterns such as (a) the Higgs dataset, using a fully connected network of size 28-300-300-300-1 (b) the MNIST dataset, with a convolutional network (ConvNet) LeNet-5 [54] and (c) the CIFAR-10 dataset, also with (ConvNet) LeNet-5. Taken from [15].

We first learn the HIGGS dataset [51] with a fully connected architecture. After 100 epochs, our model reaches classification test errors (mean \pm std) of (27.6 ± 0.4) % on par with a standard ANN trained using stochastic gradient descent and BP at (27.8 ± 0.4) %. But since GLE does not assume any specific connectivity pattern, we can make use of different deep network topologies. Here we demonstrate this by introducing convolutional architectures on both the standard MNIST dataset [52] and the more challenging CIFAR10 [53] datasets. On these datasets, our networks achieve test errors of (1.1 ± 0.1) % (MNIST) and (38.0 ± 1.3) % (CIFAR10), again on par with ANNs with identical structure at (1.08 ± 0.07) % (MNIST) and (39.4 ± 5.6) % (CIFAR10). Thus, as an extension of LE, GLE naturally maintains its predecessor’s competitive capabilities for online learning of spatial tasks.

4 Discussion

4.1 Connection to related approaches

GLE sits at the crossroads of many approaches that intend to account for temporal processing in neural networks in a biologically plausible way. As an extension of LE, it is firmly rooted on an energy-based paradigm. But there are also less obvious connections to other methods that have been proposed in the literature. We discuss some of these below.

4.1.1 LE

GLE can be seen as the spiritual successor of LE. As stated above, it inherits from LE its energy-based approach, where the whole dynamics is derived from a procedure of energy minimization. GLE also builds on the LE insight that prospective coding can undo the low-pass filtering of the neuronal membrane. What distinguishes GLE is its use of a spatio-temporal (instead of just spatial) cost function, requiring qualitatively different, “temporally aware” errors, which in turn introduce the need for more flexible prospective coding. As opposed to the case $\tau^m = \tau^r$ that characterizes LE, GLE relaxes this constraint in order to allow for memory effects, and for compensating the effects of delayed transmission on the errors. This in turn requires the time scales to be swapped when constructing errors, as discussed in detail above.

Because LE can be seen as a limit case of GLE, the new method explains *post facto* the effectiveness of LE, and also answers some of the questions left open by the older formalism. Indeed, the GLE analysis demonstrates that LE is an *exact* implementation of the Adjoint Method in the case of equal time constants, something that confirms the good grounding of the method, and helps explain its proven effectiveness. Conversely, we can show that when $\tau^m \sim \tau^r$ GLE evolves towards LE when via the adaptation of the time constants when required by task to which the framework is applied. This provides an explanation of how the coincidence of time-scales required by LE could realistically emerge in the first place, adding robustness to the method.

We thus conclude that GLE not only extends LE to more general classes of problems, but also provides it with a better theoretical grounding, and with increased biological plausibility. At the same time, the quality of the results shown by LE provides GLE with some excellent credentials, and with a great baseline for practical implementations in silico.

4.1.2 RTRL and its approximations

The Real-Time Recurrent Learning (RTRL) [55] algorithm implements online learning by storing the past states of the network in memory, and using them to calculate the influence that past neuronal activities and synaptic weights have on current neuronal activities. Unfortunately, implementing RTRL requires storing $\mathcal{O}(n^3)$ floating-point numbers in memory, and performing $\mathcal{O}(n^4)$ operations when updating the weights, neither being reasonably efficient nor biologically plausible. Nonetheless, several approximations of RTRL have been proposed recently, some of which are biologically plausible. One such algorithm is Random-Feedback Online Learning (RFLO) [56], in which an eligibility trace is used to find an approximation of the loss gradient that implements a low-pass filter with a network time constant on past influences to the activity.

RFLO is close in spirit to GLE, albeit with some notable differences which we consider to give GLE both a conceptual and a practical advantage. First, in RFLO the neurons and synapses are assumed to share time constants, in order for the filtering of the past activity to be consistent in the forward and backward passes. While not impossible, this would require the particular neurophysiological coincidence of synaptic eligibility trace biochemistry closely matching the time constants of efferent neuronal membranes. We argue that this at least reduces the biological plausibility of this approximation. In contrast, in GLE the symmetry requirements are rather between neurons, which belong to the same class of neurophysiological objects, and their time constants can be learned locally within the framework of GLE. A further property that puts RFLO at a disadvantage is its simplified tensor structure. While allowing it to scale with only n^2 , it also implies that RFLO only carries information about first-order synaptic interactions. This is in contrast to GLE, which can deal with much longer error chains, albeit in an approximated way. This flexibility allows GLE to cover applications over multiple time scales, from purely spatial classification (quasi-instantaneous reaction) to slow temporal classification. Moreover, GLE accomplishes this within a biologically plausible, mechanistic model of error transmission in cortical microcircuits. Finally, GLE compute requirements only scale quadratically with the number of neurons, which by itself represents a significant advantage over several of these other methods.

4.1.3 Locally recurrent neural networks

GLE networks can be seen as a specific case of Locally Recurrent Neural Networks (LRNNs, see, e.g., [57]). The recurrence in these networks is far more limited than in standard recurrent neural networks, and happens at the level of a single layer. Explicitly, each GLE leaky integrator neuron can be interpreted as being a special case of such a LRN.

In recent years there has been renewed interest in LRNNs, in the form of Local Recurrent Units (LRUs) as described in [58, 59]. LRUs combine the fast inference characteristics of LRNNs with ease of training and stability stemming from their use of linear and exponential recurrences. These architectures have shown performance surpassing that of transformers in language tasks involving long sequences of tokens. With recent theoretical contributions such as [60] and practical applications such as the recently developed Mamba [61] and Griffin [62] algorithms, this represents a highly active area of machine learning research.

GLE can in fact be seen as a special case of a LRU using diagonal linear layers, where the recurrence only acts locally at the level of each neuron, and with leaky integrator dynamics playing the role of the exponential recurrences. This could open an interesting application area for analog neuromorphic devices that offer highly efficient physical implementations of these dynamics. In contrast to GLE, LRUs are also characterized by their use of complex numbers in the linear operators. An extension of GLE to complex activities seems quite feasible, by extending the temporal prospective and retrospective operators to second order in time.

4.1.4 Neurophysiology

GLE combines the power of methods such as BPTT with biological plausibility in terms of local learning rules and online learning. These features also make GLE into a promising blueprint for neuromorphic devices.

As the core feature of the model, prospective coding in biological neurons is supported by considerable experimental and theoretical evidence [18–20, 27–30] on both short and long time scales. GLE further predicts functional aspects of pyramidal (PYR) neuron morphology, as well as cortical microcircuits (CMCs) for signal and error propagation. In these CMCs, pyramidal cells are responsible for the transmission of both representation and error signals, as supported by ample experimental data [32–37]. Furthermore, by representing forward activities and backward errors in separate pathways, these CMCs are capable of robust learning.

While building on many insights from previous proposals for CMCs, most notably [63], we argue that our proposed model features significant improvements. Our model does not require two kinds of nerve cells to closely track each others' activity (VIP interneurons and PYR cells), which is more easy to reconcile with the known electrophysiology of cortical neurons. This also makes training more robust and obviates the need to copy neuronal activities when training the network for more complex tasks.

Additionally, alternative models of CMCs for error backpropagation suffer from a relaxation problem, as already addressed in [15]. As it subsumes the capabilities of LE, GLE is inherently able to alleviate this problem. Of course, this also implies that alternative CMC models are only capable of dealing with purely spatial classifications. We have shown that GLE can perform spatial and temporal tasks across a range of scales.

5 Conclusions

With Generalized Latent Equilibrium, we have proposed a new framework for inference and learning of complex spatio-temporal tasks in physical systems. GLE rests on four simple postulates: prospective coding as observed in biological neurons, the formulation of a neuronal mismatch energy, a form of energy conservation under neuronal dynamics and gradient descent on the energy for synaptic plasticity. This has allowed us to provide a plausible answer to the spatiotemporal credit assignment problem in physical networks, in contrast to classical AM/BPTT, but still rivaling its performance.

As we have shown, the GLE dynamics provides an efficient on-line approximation of AM/BPTT. Thus, GLE networks can achieve results competitive with well-known, powerful machine learning architectures such as Gated Recurrent Units and Temporal Convolutional Networks. Notably, this is done with fully local, always-on, phase-free learning in real time, making it a promising candidate for realizing efficient bio-plausible online learning of spatiotemporal input streams in analog physical systems, both biological and artificial.

Our framework carries implications both for neuroscience and for the design of neuromorphic hardware. For the brain, GLE fundamentally extends previous insights about how inference and learning can operate, by leveraging an interplay between retrospective and prospective coding at the neuronal level. For artificial implementations, its underlying mechanics and demonstrated capabilities may constitute powerful assets in the context of autonomous learning on low-power neuromorphic devices.

6 Acknowledgements

We gratefully acknowledge funding from the European Union for the Human Brain Project under the grant agreement 945539, the Manfred Stärk Foundation, the Swiss National Science Foundation (SNSF) for the Grant “Prospective coding with pyramidal neurons” (310030L 156863) and the Sinergia Grant “Neural Processing of Distinct Prediction Errors: Theory, Mechanisms & Interventions” (CR-SII5 180316). Our work has greatly benefitted from access to the Fenix Infrastructure resources, which are partially funded from the European Union’s Horizon 2020 research and innovation programme through the ICEI project under the grant agreement No. 800858. Furthermore, we thank Marcel Affolter, Reinhard Dietrich and the Insel Data Science Center for the usage and outstanding support of their Research HPC Cluster.

References

1. Baydin, A. G., Pearlmutter, B. A., Radul, A. A. & Siskind, J. M. Automatic Differentiation in Machine Learning: A Survey. *Journal of Machine Learning Research* **18**, 1–43. ISSN: 1533-7928 (2018).
2. Pearlmutter, B. Gradient Calculations for Dynamic Recurrent Neural Networks: A Survey. *IEEE Transactions on Neural Networks* **6**, 1212–1228. ISSN: 1941-0093 (Sept. 1995).
3. Linnainmaa, S. Taylor Expansion of the Accumulated Rounding Error. *BIT Numerical Mathematics* **16**, 146–160. ISSN: 1572-9125 (June 1976).
4. Werbos, P. J. Applications of Advances in Nonlinear Sensitivity Analysis. *Proc. IFIP* (eds Drenick, R & Kozin, F) (1982).

5. Rumelhart, D. E., Hinton, G. E. & Williams, R. J. Learning Representations by Back-Propagating Errors. *Nature* **323**, 533–536. ISSN: 1476-4687 (Oct. 1986).
6. Pineda, F. J. Generalization of Back-Propagation to Recurrent Neural Networks. *Physical Review Letters* **59**, 2229–2232 (Nov. 1987).
7. Werbos, P. Backpropagation through Time: What It Does and How to Do It. *Proceedings of the IEEE* **78**, 1550–1560. ISSN: 1558-2256 (Oct. 1990).
8. Kelley, H. J. in *Mathematics in Science and Engineering* 205–254 (Elsevier, 1962).
9. Todorov, E. in *The Bayesian Brain* (eds Doya, K., Ishii, S., Pouget, A. & Rao, R. P.) 12: 1–28 (MIT Press, 2006).
10. Chachuat, B. Nonlinear and Dynamic Optimization: From Theory to Practice. *Lecture notes, EPFL*, 1–187. <https://infoscience.epfl.ch/record/111939> (2007).
11. Sutton, R. *Reinforcement learning* 2nd (MIT Press, 2018).
12. DePasquale, B., Cueva, C. J., Rajan, K., Escola, G. S. & Abbott, L. F. Full-FORCE: A Target-Based Method for Training Recurrent Networks. *PLOS ONE* **13**, e0191527. ISSN: 1932-6203 (Feb. 2018).
13. Gilra, A. & Gerstner, W. Predicting Non-Linear Dynamics by Stable Local Learning in a Recurrent Spiking Neural Network. *eLife* **6** (ed Latham, P.) e28295. ISSN: 2050-084X (Nov. 2017).
14. Marschall, O., Cho, K. & Savin, C. A Unified Framework of Online Learning Algorithms for Training Recurrent Neural Networks. *Journal of Machine Learning Research* **21**, 1–34. ISSN: 1533-7928 (2020).
15. Haider, P. et al. *Latent Equilibrium: A Unified Learning Theory for Arbitrarily Fast Computation with Arbitrarily Slow Neurons* in *Advances in Neural Information Processing Systems* **34** (Curran Associates, Inc., 2021), 17839–17851.
16. Hodgkin, A. L. & Huxley, A. F. A Quantitative Description of Membrane Current and Its Application to Conduction and Excitation in Nerve. *The Journal of Physiology* **117**, 500–544. ISSN: 0022-3751 (Aug. 1952).
17. Köndgen, H. et al. The Dynamical Response Properties of Neocortical Neurons to Temporally Modulated Noisy Inputs In Vitro. *Cerebral Cortex* **18**, 2086–2097. ISSN: 1047-3211 (Sept. 2008).
18. Plesser, H. E. & Gerstner, W. Escape Rate Models for Noisy Integrate-and-Free Neurons. *Neurocomputing* **32–33**, 219–224. ISSN: 0925-2312 (June 2000).
19. Pozzorini, C., Naud, R., Mensi, S. & Gerstner, W. Temporal whitening by power-law adaptation in neocortical neurons. *Nature neuroscience* **16**, 942–948 (2013).
20. Brandt, S., Benitez, F., Petrovici, M. A., Senn, W. & Wilmes, K. Prospective and retrospective coding in cortex and hippocampus. *In preparation* (2024).
21. Izhikevich, E. M. Simple model of spiking neurons. *IEEE Transactions on neural networks* **14**, 1569–1572 (2003).
22. Brette, R. & Gerstner, W. Adaptive exponential integrate-and-fire model as an effective description of neuronal activity. *Journal of neurophysiology* **94**, 3637–3642 (2005).
23. Billaudelle, S., Weis, J., Dauer, P. & Schemmel, J. *An accurate and flexible analog emulation of AdEx neuron dynamics in silicon* in *2022 29th IEEE International Conference on Electronics, Circuits and Systems (ICECS)* (2022), 1–4.
24. Hopfield, J. J. Neural Networks and Physical Systems with Emergent Collective Computational Abilities. *Proceedings of the National Academy of Sciences* **79**, 2554–2558 (Apr. 1982).
25. Ackley, D. H., Hinton, G. E. & Sejnowski, T. J. A Learning Algorithm for Boltzmann Machines*. *Cognitive Science* **9**, 147–169. ISSN: 0364-0213, 1551-6709 (Jan. 1985).
26. Scellier, B. & Bengio, Y. Equilibrium Propagation: Bridging the Gap Between Energy-Based Models and Backpropagation. *arXiv:1602.05179 [cs]*. arXiv: 1602.05179 [cs] (Mar. 2017).
27. Mainen, Z. F., Joerges, J., Huguenard, J. R. & Sejnowski, T. J. A model of spike initiation in neocortical pyramidal neurons. en. *Neuron* **15**, 1427–1439. ISSN: 08966273. <https://linkinghub.elsevier.com/retrieve/pii/S0896627395900209> (2022) (Dec. 1995).

28. Gerstner, W., Kistler, W. M., Naud, R. & Paninski, L. *Neuronal Dynamics: From Single Neurons to Networks and Models of Cognition* 1st ed. ISBN: 9781107060838 9781107635197 9781107447615. <https://www.cambridge.org/core/product/identifier/9781107447615/type/book> (2024) (Cambridge University Press, July 2014).
29. Traub, R. D. & Miles, R. *Neuronal Networks of the Hippocampus* 1st ed. ISBN: 9780521364812 9780521063319 9780511895401. <https://www.cambridge.org/core/product/identifier/9780511895401/type/book> (2024) (Cambridge University Press, May 1991).
30. Brette, R. et al. Simulation of networks of spiking neurons: A review of tools and strategies. en. *Journal of Computational Neuroscience* **23**, 349–398. ISSN: 1573-6873. <http://link.springer.com/10.1007/s10827-007-0038-6> (2022) (Dec. 2007).
31. Urbanczik, R. & Senn, W. Learning by the dendritic prediction of somatic spiking. *Neuron* **81**, 521–528 (2014).
32. Zmarz, P. & Keller, G. B. Mismatch receptive fields in mouse visual cortex. *Neuron* **92**, 766–772 (2016).
33. Fiser, A. et al. Experience-dependent spatial expectations in mouse visual cortex. *Nature neuroscience* **19**, 1658–1664 (2016).
34. Attinger, A., Wang, B. & Keller, G. B. Visuomotor coupling shapes the functional development of mouse visual cortex. *Cell* **169**, 1291–1302 (2017).
35. Keller, G. B. & Mrsic-Flogel, T. D. Predictive Processing: A Canonical Cortical Computation. *Neuron* **100**, 424–435. ISSN: 08966273. (2024) (Oct. 2018).
36. Ayaz, A. et al. Layer-specific integration of locomotion and sensory information in mouse barrel cortex. *Nature communications* **10**, 2585 (2019).
37. Gillon, C. J. et al. Responses to pattern-violating visual stimuli evolve differently over days in somata and distal apical dendrites. *Journal of Neuroscience* **44** (2024).
38. Wilson, N. R., Runyan, C. A., Wang, F. L. & Sur, M. Division and subtraction by distinct cortical inhibitory networks in vivo. *Nature* **488**, 343–348 (2012).
39. Seybold, B. A., Phillips, E. A., Schreiner, C. E. & Hasenstaub, A. R. Inhibitory actions unified by network integration. *Neuron* **87**, 1181–1192 (2015).
40. Lee, S., Kruglikov, I., Huang, Z. J., Fishell, G. & Rudy, B. A disinhibitory circuit mediates motor integration in the somatosensory cortex. *Nature neuroscience* **16**, 1662–1670 (2013).
41. Dorsett, C., Philpot, B. D., Smith, S. L. & Smith, I. T. The impact of SST and PV interneurons on nonlinear synaptic integration in the neocortex. *Eneuro* **8** (2021).
42. Petrovici, M. A. Form versus function: theory and models for neuronal substrates. **1** (2016).
43. Lillicrap, T. P., Cownden, D., Tweed, D. B. & Akerman, C. J. Random Feedback Weights Support Learning in Deep Neural Networks. *arXiv:1411.0247 [cs, q-bio]*. arXiv: 1411.0247 [cs, q-bio] (Nov. 2014).
44. Max, K. et al. *Learning Efficient Backprojections Across Cortical Hierarchies in Real Time in Artificial Neural Networks and Machine Learning – ICANN 2023* (eds Iliadis, L., Papaleonidas, A., Angelov, P. & Jayne, C.) (Springer Nature Switzerland, Cham, 2023), 556–559. ISBN: 978-3-031-44207-0.
45. Gierlich, T. et al. Weight transport through spike timing for robust local gradients (in prep.).
46. Greydanus, S. *Scaling down Deep Learning* Dec. 2020. arXiv: 2011.14439 [cs, stat].
47. Bai, S., Kolter, J. Z. & Koltun, V. *An Empirical Evaluation of Generic Convolutional and Recurrent Networks for Sequence Modeling* 2018. arXiv: 1803.01271 [cs.LG].
48. Cho, K. et al. *Learning Phrase Representations using RNN Encoder-Decoder for Statistical Machine Translation* 2014. arXiv: 1406.1078 [cs.CL].
49. Warden, P. *Speech Commands: A Dataset for Limited-Vocabulary Speech Recognition* 2018. arXiv: 1804.03209 [cs.CL].
50. Zhang, Y., Suda, N., Lai, L. & Chandra, V. *Hello Edge: Keyword Spotting on Microcontrollers* 2018. arXiv: 1711.07128 [cs.SD].

51. Baldi, P., Sadowski, P. & Whiteson, D. Searching for exotic particles in high-energy physics with deep learning. *Nature communications* **5**, 4308 (2014).
52. LeCun, Y., Bottou, L., Bengio, Y. & Haffner, P. Gradient-based learning applied to document recognition. *Proceedings of the IEEE* **86**, 2278–2324 (1998).
53. Krizhevsky, A., Hinton, G., et al. Learning multiple layers of features from tiny images (2009).
54. LeCun, Y. et al. Backpropagation applied to handwritten zip code recognition. *Neural computation* **1**, 541–551 (1989).
55. Williams, R. J. & Zipser, D. in *Backpropagation: Theory, Architectures, and Applications* 433–486 (Lawrence Erlbaum Associates, Inc, Hillsdale, NJ, US, 1995). ISBN: 978-0-8058-1258-9 978-0-8058-1259-6.
56. Murray, J. M. Local Online Learning in Recurrent Networks with Random Feedback. *eLife* **8**, e43299. ISSN: 2050-084X (May 2019).
57. Campolucci, P., Uncini, A. & Piazza, F. *Causal Back Propagation through Time for Locally Recurrent Neural Networks in 1996 IEEE International Symposium on Circuits and Systems. Circuits and Systems Connecting the World. ISCAS 96* **3** (May 1996), 531–534 vol.3.
58. Orvieto, A. et al. *Resurrecting Recurrent Neural Networks for Long Sequences* in *Proceedings of the 40th International Conference on Machine Learning* (PMLR, July 2023), 26670–26698.
59. Orvieto, A., De, S., Gulcehre, C., Pascanu, R. & Smith, S. L. *Universality of Linear Recurrences Followed by Non-linear Projections: Finite-Width Guarantees and Benefits of Complex Eigenvalues* Mar. 2024. arXiv: 2307.11888 [cs].
60. Zucchet, N., Meier, R., Schug, S., Mujika, A. & Sacramento, J. *Online Learning of Long-Range Dependencies* May 2023. arXiv: 2305.15947 [cs].
61. Gu, A. & Dao, T. *Mamba: Linear-Time Sequence Modeling with Selective State Spaces* Dec. 2023. arXiv: 2312.00752 [cs].
62. De, S. et al. *Griffin: Mixing Gated Linear Recurrences with Local Attention for Efficient Language Models* Feb. 2024. arXiv: 2402.19427 [cs].
63. Sacramento, J., Ponte Costa, R., Bengio, Y. & Senn, W. *Dendritic Cortical Microcircuits Approximate the Back-propagation Algorithm* in *Advances in Neural Information Processing Systems* **31** (Curran Associates, Inc., 2018).